Glucosamine sulphate-loaded distearoyl phosphocholine liposomes for osteoarthritis treatment: combination of sustained drug release and improved lubrication

Xiuling Ji‡ a, Yufei Yan‡ b, Tao Sun a, Qiang Zhang c, Yixin Wang a, Ming Zhang c, Hongyu Zhang *a and Xin Zhao*c

aState Key Laboratory of Tribology, Department of Mechanical Engineering, Tsinghua University, Beijing 100084, China. E-mail: zhanghyu@tsinghua.edu.cn; Fax: +86 010 62781379; Tel: +86 010 62796053
bShanghai Key Laboratory for Prevention and Treatment of Bone and Joint Diseases, Shanghai Institute of Traumatology and Orthopaedics, Ruijin Hospital, Shanghai Jiao Tong University School of Medicine, Shanghai 200025, China
cDepartment of Biomedical Engineering, The Hong Kong Polytechnic University, Hung Hom, Hong Kong SAR, China. E-mail: xin.zhao@polyu.edu.hk; Tel: +852 3400 8083

Abstract
Osteoarthritis (OA) is a chronic joint disease resulting from joint inflammation and damage. In this study, we employed a boundary lubricant known as a 1,2-distearoyl-sn-glycero-3-phosphocholine (DSPC) liposome for loading of an anti-inflammatory drug D-glucosamine sulphate (GAS) to construct a treatment strategy allowing for sustained anti-inflammation and reduced damage. This kind of drug-loaded nanocarrier integrates the anti-inflammatory effect of the GAS and the lubrication ability of DSPC liposomes without the involvement of complex synthesis processes leading to easier popularization. Our experimental results indicated that the GAS-loaded DSPC liposomes could release GAS in a sustained manner while providing good lubrication in pure water (H2O) and phosphate buffered saline (PBS). Moreover, the GAS-loaded DSPC liposomes prepared at a 2[thin space (1/6-em)]:[thin space (1/6-em)]8 molar ratio in PBS exhibited a greater entrapment efficiency, lower GAS release rate and smaller friction coefficient as compared to those prepared in H2O. The superiority of the drug release and lubrication ability achieved with the GAS-loaded DSPC liposomes in PBS were elucidated on the basis of salt-induced enhancement in liposomal stability and hydration lubrication by the hydrated salt ions. Such GAS release accelerated the viability and proliferation of primary mouse chondrocytes while also providing the anti-inflammatory and chondroprotective potential for tumor necrosis factor (TNF-α) induced chondrocyte degeneration through the down-regulation of pro-inflammatory cytokines, pain related gene and catabolic proteases, as well as the up-regulation of anabolic components. We envision that the GAS-loaded DSPC liposomes could represent a promising new strategy for clinical treatment of OA in the future.

1. Introduction

From a biotribological point of view, osteoarthritis (OA) has been regarded as a friction-related joint disease resulting from inflammation and cartilage degeneration.1 Moreover, it is a well-known fact

that cartilage degeneration is closely related to high friction and wear at the joints. For this reason, the target of treatment for OA is to reduce the joint inflammation together with high friction and wear while maintaining its function. Meanwhile, therapeutics such as anti-inflammatory drugs can alleviate joint inflammation, while lubrication can reduce friction and wear by separating opposing surfaces with a fluid film or boundary layer. To improve the therapeutic efficacy of OA, treatments integrating both sustained anti-inflammation and improved lubrication have been in ever-increasing need.

Among the current OA treatment methods, local intra-articular drug delivery is a more effective method compared to oral drug delivery, due to its reduced systemic toxicity. Unfortunately, direct drug administration via intra-articular injections suffers from disadvantages as well, including the short residence time of drugs and a high concentration of drugs in the joint capsules.2 Therefore, in order to improve the therapeutic efficacy of intra-articularly injected drugs, the incorporation of anti-inflammatory drugs within carriers to achieve a sustained drug release over a prolonged period has been developed.3 The usage of drug carriers in intra-articular drug administration allows for specific and sustained drug targeting to the damaged tissues with fewer side effects.4 The carriers currently used include liposomes5–9 and nano-/microparticles made of biodegradable polymers10–14 or mesoporous silica.15–21 In the case of nano-/microparticles, a range of polymer-based nano-/microparticles have been reported as drug carriers. However, most of these particles suitable for the intra-articular drug delivery are difficult to popularize, because the sustained release of incorporated drugs in the drug delivery systems can merely be achieved with drugs that have a high affinity for polymer-based nano-/microparticles.22 To improve the drug affinity to carriers and control the degree of drug release, nano-/microparticles based on polymer–drug conjugates have been developed.23 Liu et al.10 constructed polymer-based nanomicelles by chemically binding curcumin to hyaluronic acid. For mesoporous silica nanoparticles (MSNs) with large drug loading capacity due to their highly ordered mesoporous structure and large surface area, they may introduce abrasion and destroy joint lubrication, accelerating the OA development upon intra-articular injection.24 To improve their lubrication ability, various lubricating materials such as poly(2-methacryloyloxyethyl phosphorylcholine) (PMPC) or distearoyl phosphatidylcholine (DSPC) can be grafted onto the surfaces of MSNs.25,26 Nevertheless, surface modification of MSNs involves complicated synthesis procedures which may introduce toxic chemicals during the synthetic process, making modified MSNs difficult to popularize. Due to the difficulty in popularization, liposomes formed by biocompatible phospholipids are proposed for intra-articular drug delivery. Specifically, phosphatidylcholine liposomes can work not only as drug carriers, but also as extremely efficient lubricating agents to reduce friction for prolonged periods of time in aqueous systems.27–29 When phosphatidylcholine liposomes are used as drug carriers for intra-articular administration, efficient entrapment of both lipophilic and hydrophilic drugs can be achieved. Moreover, they are self-lubricating materials with their lubrication ability attributed to the hydration layers surrounding the zwitterionic headgroups. The water molecules in the hydration layers work in a ball-bearing-like manner, causing friction reduction and lubrication enhancement of the liposomes.30 Accordingly, phosphatidylcholine liposomes integrate drug delivery and lubrication properties without tedious synthesis steps, allowing for easy popularization while making a more facile and effective attempt at intra-articular drug administration for OA treatment. Unfortunately, certain unstable phosphatidylcholine liposomes spontaneously rupture and produce lipid bilayers when being adsorbed onto the surface, whereas the immobilization onto the joint surface is a prerequisite for

providing sustained drug release and acting as efficient boundary lubricants.31,32 It is therefore imperative to select stable liposomes for intra-articular drug administration to avoid liposome rupture and premature leakage of loaded drugs while improving lubrication as surface-bound intact liposomes.

In this study, we fabricated a self-lubricating drug delivery system composed of D-glucosamine sulphate (GAS) and 1,2-distearoyl-sn-glycero-3-phosphocholine (DSPC) liposomes. GAS stimulates proteoglycan and collagen synthesis of the extracellular matrix (ECM) of cartilage. Moreover, GAS inhibits the activity of pain related gene and matrix metalloproteinases (MMPs), decreases the level of pro-inflammatory cytokine secretion, and thus has been used extensively as an anti-inflammatory and chondroprotective drug for OA treatment.33–36 Normally, GAS is used as an oral drug, and the commonly prescribed oral dose is 500 mg taken three times in a day. However, the oral administration has only 10–20% bioavailability and insignificant therapeutic efficacy due to trace amounts of GAS entering the joint cavity.33 The GAS maximum level in synovial fluid is in the order of micromoles by the oral route, which is much lower than the achieved level with the intravenous administration. DSPC liposomes are used in the present study as they are formed by lipids bearing two long chain C18 acyl chains, which contribute to the great stability and the formation of surface-bound intact liposomes.37,38 Other liposomes like hydrogenated soy phosphatidylcholine (HSPC) can also be used for the drug release and lubrication purposes as they do not spontaneously rupture to produce lipid bilayers and form surface-bound intact liposomes on the surface. We anticipate that our DSPC–GAS liposomes will provide efficient boundary lubrication at the joint surface while simultaneously releasing GAS at a slow and sustained rate. To obtain the maximum entrapment efficiency, the optimization of DSPC liposomes for GAS delivery was first performed by altering their molar ratios. Then the drug release behaviors and lubrication properties of DSPC–GAS liposomes at the optimum molar ratio in two different media including pure water (H_2O) and phosphate buffered saline (PBS) at 37 °C were studied. It was found that there was a greater entrapment efficiency, lower release rate of GAS and a smaller friction coefficient of DSPC–GAS liposomes. These results were obtained with PBS due to the salt-induced enhancement in liposomal stability and hydration lubrication by hydrated salt ions. Additionally, the released GAS accelerated the viability and proliferation of primary mouse chondrocytes. In the case of the primary mouse chondrocytes treated with tumor necrosis factor (TNF-α), it provided anti-inflammatory and chondroprotective potential. Without the consideration of drug affinity and complicated synthesis procedures, our simple and biocompatible DSPC–GAS liposomes endow self-lubricating drug carriers bearing sustained drug release and improved lubrication properties. We envision that the DSPC–GAS liposomes will have clinical potential for the treatment of OA, as shown in Scheme 1.

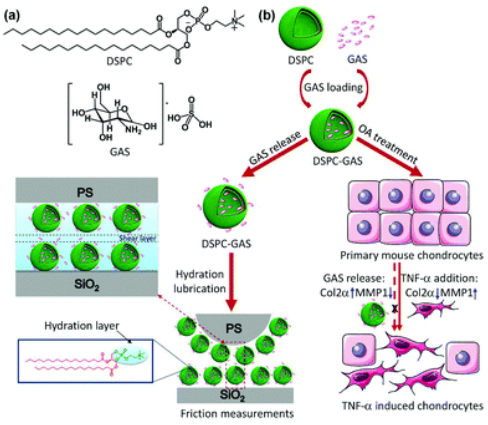

Scheme 1 Simplified model of the preparation and characterization of DSPC–GAS liposomes integrating sustained drug release and improved lubrication. (a) The chemical structures of DSPC and GAS. (b) Schematic diagram of the preparation, drug release and lubrication of DSPC–GAS liposomes, as well as their anti-inflammatory and chondroprotective potential in primary mouse chondrocytes treated with TNF-α.

2. Materials and methods

2.1. Materials

DSPC (>95.0% purity) was purchased from TCI Co., Ltd (Shanghai, China) and used as received. Cholesterol (95.0% purity) was purchased from J&K Scientific Chemical Reagent Co., Ltd (Beijing, China). GAS (98% purity), PBS and polystyrene microspheres (PS, 5% w/v) with a diameter of 4.0–4.9 μm were purchased from Aladdin Co. (Shanghai, China). Potassium ferricyanide (K3Fe(CN)6, ≥99.5% purity) was purchased from Solarbio Biotech Co., Ltd (Beijing, China). Sodium hydroxide (NaOH, ≥96% purity) was purchased from Modern Oriental Technology Development Co., Ltd (Beijing, China). Methanol (99.5% purity, AR grade) and chloroform (99.5% purity, AR grade) were obtained from Sinopharm Chemical Reagent Co., Ltd (Beijing, China). The type of 'TL-CONT' tipless AFM cantilever probe was purchased from NanoWorld AG (Headquarters, Switzerland). P-Doped, (100)-oriented silicon wafers (1–10 Ω·cm resistivity, 950 μm thickness, 10 mm × 10 mm) were purchased from Haisi Co. (Linyi, China). The water used in these experiments was Milli-Q water (18.2 MΩ cm).

2.2. Preparation of DSPC–GAS liposomes

DSPC–GAS liposomes were prepared by the thin film hydration method.39 DSPC and cholesterol with a 4[thin space (1/6-em)]:[thin space (1/6-em)]1 mass ratio were dissolved in a mixture of methanol–chloroform (85[thin space (1/6-em)]:[thin space (1/6-em)]15, v/v) and sonicated for 10 min to ensure complete dissolution. A rotary evaporator was used under vacuum at 60 °C to remove the solvent from the resulting homogeneous samples and obtain a thin lipid film. Next, the thin lipid film was hydrated with GAS solution and thermostated for 1 h at the temperature above the DSPC phase transition temperature of 60 °C to form multilamellar liposomes. After that, the multilamellar liposomes were downsized to form small unilamellar liposomes by extruding successively using an extruder (Avanti, USA) through polycarbonate membranes (Whatman, Inc.) with a defined pore size of 400 nm (11 cycles) and 100 nm (11 cycles). It should be mentioned here that the temperature was maintained at 60 °C during the whole extrusion process. The optimization of DSPC–GAS liposomes was performed by altering the molar ratios of DSPC and GAS while simultaneously maintaining the DSPC concentration. The final concentration of the DSPC–GAS liposomes was chosen at 5.0

mM when taken into consideration the smaller friction coefficient and the larger loading capacity (Fig. S1†).

2.3. GAS encapsulation efficiency and release

The DSPC–GAS liposomes prepared by the thin film hydration method were centrifuged at 25[thin space (1/6-em)]000g × 10 min at 4 °C. The amount of GAS remaining in the supernatant was analyzed through the employment of a UV-6100A spectrophotometer (Metash Instruments, China) at a wavelength of 420 nm. The concentration corresponding to the absorbance was determined from the calibration curve for GAS. The GAS calibration curve in H2O and PBS (Fig. S2†) was obtained as previously reported.40 The drug loading capacity (LC, %) and the encapsulation efficiency (EE, %) were then calculated by the following equations respectively.

$$\mathrm{LC}(\%) = \frac{\text{Amount of added GAS} - \text{amount of GAS in supernatant}}{\text{Amount of GAS-loaded DSPC}} \times 100$$

$$\mathrm{EE}(\%) = \frac{\text{Amount of added GAS} - \text{amount of GAS in supernatant}}{\text{Amount of added GAS}} \times 100$$

The release of GAS from the DSPC–GAS liposomes in H2O and PBS was studied with the dialysis method. This method involved inputting 1 mL of DSPC–GAS liposomes in a dialysis tube (molecular weight cutoff: 1000) which was placed in 40 mL release medium (H2O and PBS) under constant stirring at 15 rpm. The experiment was performed in triplicate at 37 °C. After a predetermined time point, 1 mL of the release medium was withdrawn and replaced by an equal volume of fresh medium. The amount of GAS released from DSPC–GAS liposomes was evaluated by using a UV-6100A spectrophotometer.

2.4. Characterization of DSPC–GAS liposomes

The DSPC–GAS liposomes prepared with the molar ratio of 2[thin space (1/6-em)]:[thin space (1/6-em)]8 at 5.0 mM DSPC concentration in H2O and PBS were dialyzed in the corresponding medium for 24 h via a dialysis tube (molecular weight cutoff: 1000). Then, the hydrodynamic diameters and zeta potentials of the obtained DSPC–GAS liposomes in two separate media were measured with a Malvern Zetasizer Nano-ZS size instrument (Malvern Instruments, Malvern, UK) at 37 °C. Their morphologies were imaged by using a field-emission scanning electron microscope (SEM, Quanta 200, Eindhoven, Netherlands). To maintain the original structures and morphologies of the formed DSPC–GAS liposomal layers, DSPC–GAS liposomes were adsorbed on silicon wafers for 30 min and were then rinsed with pure water before freezing at −180 °C by liquid nitrogen. Afterwards, the frozen samples were lyophilized under vacuum at about −80 °C. Lastly, the lyophilized samples were coated with 1–2 nm Pt.

2.5. Friction measurements

The friction measurements were performed using an Asylum Research MFP-3D AFM in contact mode. A rectangular tipless cantilever (TL-CONT) with a nominal spring constant (KN) with a range from 0.02 to 0.77 N m−1 (the exact value of KN was determined by the frequency method41) was used. Then, the epoxy glue was utilized to attach the polystyrene microsphere to the cantilever end,

and attach the silicon wafer onto a clean fluid cell. Furthermore, the DSPC–GAS liposomes in H2O or PBS were injected into the fluid cell and incubated for 30 min, and the non-adsorbed DSPC–GAS liposomes were rinsed with their corresponding medium. After rinsing, an adsorbed layer composed of the remaining DSPC–GAS liposomes was formed onto the silicon wafer. The lateral force measurements were then conducted between the silica surface bearing an adsorbed layer and the polystyrene surface in H2O or PBS. During the lateral force measurement, the colloidal probe was pressed against the silicon wafer at a constant applied load, while the silicon wafer slid horizontally underneath the cantilever. The lateral scanning area of each friction region was set to 20 μm × 5 μm, and the scanning rate was set as 2.00 Hz. Exceptions can be found in cases where the effect of the scanning rate was considered. The lateral force (FL) was measured under different normal loads (FN) by adjusting the applied voltage. Before each experiment, the silicon wafers were cleaned in an ultrasonic bath with acetone and a mixture of acetone–ethanol (50[thin space (1/6-em)]:[thin space (1/6-em)]50, v/v) for 10 min each, and then washed with pure water followed by drying with nitrogen gas. The colloidal probes were washed with ethanol and pure water each for 5 min sequentially. All experiments were done at 37 °C.

2.6. Cytotoxicity and protective effect for inflammation induced degeneration of chondrocytes

2.6.1. Primary mouse chondrocyte isolation. Chondrocytes (passage <3) were isolated from articular cartilage in the knee joints of mice as previously reported.42 The articular cartilage tissues were firstly cut into small pieces (1 mm3), and then these small pieces were digested with 0.25% trypsin for 30 min and 0.2% type II collagenase for 4 h, sequentially. After that, the released cells were cultured in DMEM/F12 media containing 10% fetal bovine serum and antibiotics. Note that unless otherwise explained, the DSPC–GAS liposomes used in the following tests were prepared with a 2[thin space (1/6-em)]:[thin space (1/6-em)]8 molar ratio at a DSPC concentration of 5.0 mM.

2.6.2. Cell morphology and viability. The effects of DSPC liposomes, DSPC–GAS liposomes and free GAS solution on the morphology and viability of chondrocytes were analyzed using a Live/Dead cell kit (Life Tech, USA). The primary mouse chondrocytes were cultured in 24-well plates at a density of 5 × 104 cells per mL. During incubation, the plates were maintained in a humidified atmosphere of 37 °C and 5% CO2 with the culture medium replaced every other day. After co-culturing with 5.0 mM of DSPC liposomes, DSPC–GAS liposomes or free GAS in triplicate for 1, 3 and 5 days, the cells were stained with 500 μL of Live/Dead cell dye for 15 min, and observed using fluorescence microscopy (ZEISS, Axio Imager M1, Germany). The viable cells with esterase activity appeared green, whereas the dead cells with compromised plasma membranes appeared red, as described in the manufacturer's protocol.

2.6.3. Cell proliferation. Chondrocytes were seeded and cultured using the same procedure as before. After co-culturing with 5.0 mM of DSPC liposomes, DSPC–GAS liposomes or free GAS solution in triplicate for 1, 3 and 5 days, the Cell Counting Kit-8 (CCK-8, Dojindo Kagaku, Japan) was used to investigate their effects on the proliferation of chondrocytes. Briefly, 500 μL of fresh medium and 50 μL of CCK-8 solution were added to each well and incubated for 2 h. After that, the CCK-8 mixed medium was transferred to 96-well plates in darkness. The solution absorbance was measured through employment of a microplate reader (Infinite F50, TECAN, Switzerland) at a wavelength of 450 nm.

2.6.4. QRT-PCR analysis. To further explore the protective effect of DSPC–GAS liposomes for inflammation induced chondrocyte degeneration, quantitative real-time polymerase chain reaction (QRT-PCR) was employed to analyze the expression of cartilage-specific genes. The primary mouse

chondrocytes were seeded in 6-well plates at a density of 5 × 105 cells per mL and then stimulated with 5 nM of TNF-α to induce chondrocyte degeneration. Chondrocytes treated with TNF-α served as blank groups. After that, TNF-α-induced chondrocytes were cultured with DSPC or DSPC–GAS liposomes (1.0 or 5.0 mM) for 24 h. Total RNA from chondrocytes was extracted using a TRIzol reagent (Invitrogen, USA) with reference to previous study.43 The concentration and purity of the RNA preparations were determined by measuring the absorbance of RNA at 260 and 280 nm. First-strand cDNA was synthesized using 1 μg of total RNA as a template and a RevertAid First Strand cDNA Synthesis kit (TaKaRa, Dalian, China). Then, cDNA was amplified using a SYBR Premix Ex Tag Kit (TaKaRa) and an ABI 7500 Sequencing Detection System (Applied Biosystems, Foster City, CA, USA). The QRT-PCR reactions were performed at 95 °C for 10 min and 60 °C for 1 min. In view of the fact that the pathogenesis of OA is involved in multiple factors, such as pro-inflammatory cytokines (interleukin-1β (IL-1β), IL-6), preprotachykinin 1 gene (TAC1) and matrix metalloproteinases (MMP1), inhibition of one or two of these factors may not be favorable with regard to the OA treatment efficacy. In addition, the degradation of aggrecan (Agg) and collagen II (Col2α) in ECM in response to the chondrocyte degeneration also plays a role in OA progression. Therefore, the six molecules, IL-1β, IL-6, TAC1, MMP1, Agg and Col2α, were chosen to undergo QRT-PCR analysis. The sequence of six primers was designed by a biological company (Sangon Company, China). The primer specificity was confirmed by analyzing the dissociation curve of each primer pair, and the dissociation curves were consistent during the QRT-PCR process to make sure that there was no off-target signal. Their relative mRNA expression levels were calculated by the $2^{-\Delta\Delta CT}$ method relative to β-actin mRNA expression as reported before.44 Each experiment had at least three samples and was repeated three times, and one-way analysis of variance (ANOVA) with post-hoc Tukey's multiple comparison test was used to do the statistical analysis. All values were reported as mean ± standard deviation (SD) of triple measurements of each cDNA sample. The primer sequences used for PCR were as follows: β-actin: forward, 5′-CTGTCCCTGTATGCCTCTG-3′; reverse, 5′-ATGTCACGCACGATTTCC-3′; IL-1β: forward, 5′-CAACTGTTCCTGAACTCAACTG-3′; reverse, 5′-GAAGGAAAAGAAGGTGCTCATG-3′; IL-6: forward, 5′-CTCCCAACAGACCTGTCTATAC-3′; reverse, 5′-CCATTGCACAACTCTTTTCTCA-3′; TAC1: forward, 5′-GCCCTGTTAAAGGCTCTTTATG-3′; reverse, 5′-CTTCTTTCGTAGTTCTGCATCG-3′; MMP1: forward, 5′-GAGGAAGGCGATATTGTGCTCTC-3′; reverse, 5′-CTGCTGTTGGTCCACGTCTCATC-3′; Agg: forward, 5′-TATGATGTCTACTGCTACGTGG-3′; reverse, 5′-GTAGAGGTAGACAGTTCTCACG-3′; Col2α: forward, 5′-TACTGGAGTGACTGGTCCTAAG-3′; reverse, 5′-AACACCTTTGGGACCATCTTTT-3′.

2.6.5. Immunofluorescence staining. Chondrocytes were seeded onto sterile cover slips at a density of 5 × 104 cells per well in 24-well plates, treated with 5 nM of TNF-α and cultured with 5.0 mM of DSPC, DSPC–GAS liposomes or free GAS solution. After incubation for 12 h, the chondrocytes were successively fixed in 4% paraformaldehyde for 10 min, treated with 0.1% Triton X-100 for 15 min and incubated in 3% bovine serum albumin (BSA)/PBS for 30 min at room temperature. Then, chondrocytes were incubated with a primary anti-Col2α antibody (1[thin space (1/6-em)]:[thin space (1/6-em)]200 dilution) and anti-MMP1 antibody (1[thin space (1/6-em)]:[thin space (1/6-em)]200 dilution) overnight at a temperature of 4 °C. Col2α and MMP1 were selected to perform immunofluorescence staining due to the fact that variations in their production were a manifestation of chondrocyte degeneration. To be specific, the decreased production of Col2α and/or increased

production of MMP1 were closely related to chondrocyte degeneration. After primary antibody incubation, the cells were washed with PBS and incubated with appropriate Alexa Fluor (488)-coupled secondary antibodies (Molecular Probes, Life Tech, USA, 1[thin space (1/6-em)]:[thin space (1/6-em)]400) for 1 h at room temperature. Cell nuclei were counterstained with 4,6-diamidino-2-phenylindole dilactate (DAPI, Life Tech, USA) at room temperature for 15 min in darkness. Images were acquired using laser scanning confocal microscopy (LSCM, LSM800, ZEISS, Germany).

2.6.6. Statistical analysis. The results were expressed as mean ± SD for quantitative data, and similar independent experiments were repeated at least three times with three replicates to verify the results. Statistical significance was determined using one-way ANOVA for the multiple comparison tests and a two-tailed non-paired Student's t-test for two comparison tests. The level of significance was displayed as *P < 0.05, **P < 0.01, or ***P < 0.001; #P < 0.05, ##P < 0.01, or ###P < 0.001.

3. Results and discussion

3.1. Optimization of DSPC–GAS liposome formulations

To optimize the formulation for effective GAS loading, DSPC–GAS liposomes were prepared by altering the molar ratios of DSPC and GAS. It can be seen in Table 1 that the loading capacity of DSPC–GAS liposomes decreased with the increase in the molar ratio of DSPC and GAS. In addition, the maximum amount of loaded GAS (31.3 ± 0.9%) in DSPC–GAS liposomes was observed in a molar ratio of 1[thin space (1/6-em)]:[thin space (1/6-em)]9. Meanwhile, the encapsulation efficiency was found to initially increase and then decrease by increasing the molar ratio of DSPC and GAS. The greatest encapsulation efficiency (50.1 ± 1.2%) was given by DSPC–GAS liposomes prepared with the molar ratio of 2[thin space (1/6-em)]:[thin space (1/6-em)]8 and the loading capacity (29.3 ± 1.2%) of DSPC–GAS liposomes prepared in a 2[thin space (1/6-em)]:[thin space (1/6-em)]8 molar ratio was just slightly smaller than that (31.3 ± 0.9%) in a 1[thin space (1/6-em)]:[thin space (1/6-em)]9 molar ratio. The combined results of the loading capacity and encapsulation efficiency indicated that the DSPC–GAS liposomes prepared at a 2[thin space (1/6-em)]:[thin space (1/6-em)]8 molar ratio were the optimum selection for the drug release test. With this in consideration, the molar ratio of DSPC–GAS liposomes in the following tests was chosen to be 2[thin space (1/6-em)]:[thin space (1/6-em)]8 while the DSPC concentration at 5.0 mM remained. Exceptions can be found in cases where the concentration effect was considered.

Table 1 Loading capacity (LC, %) and encapsulation efficiency (EE, %) of DSPC–GAS liposomes prepared with different molar ratios at the DSPC concentration of 5.0 mM in H_2O at 37 °C

Sample	Loading capacity (LC, %)	Encapsulation efficiency EE (%)
DSPC : GAS = 1 : 9	(31.3 ± 0.9)%	(41.2 ± 0.9)%
DSPC : GAS = 2 : 8	(29.3 ± 1.2)%	(50.1 ± 1.2)%
DSPC : GAS = 3 : 7	(14.4 ± 0.4)%	(32.0 ± 1.5)%
DSPC : GAS = 4 : 6	(8.7 ± 0.4)%	(25.3 ± 1.4)%
DSPC : GAS = 5 : 5	(4.7 ± 0.5)%	(18.2 ± 1.5)%

3.2. Characterization of DSPC–GAS liposomes in different media

Prior to discussing the drug release behaviors and lubrication properties of DSPC–GAS liposomes in two different media including H2O and PBS, we began by characterizing their size distributions and morphologies. The average hydrodynamic diameters, zeta potentials and morphologies of DSPC–GAS liposomes at the optimum molar ratio were evaluated by DLS and SEM and their representative results are presented in Fig. 1. It can be observed from Fig. 1a that the average diameter and zeta potential of DSPC–GAS liposomes in H2O were measured to be around 120 nm and 2.8 ± 0.4 mV, while the average diameter and zeta potential in PBS were around 109 nm and 1.2 ± 0.2 mV. Both were noticeably smaller than those in H2O, demonstrating the neutral nature of DSPC–GAS liposomes in PBS. Additionally, DSPC–GAS liposomes in both media showed a polydispersity (PDI) < 0.2 (H2O[thin space (1/6-em)]:[thin space (1/6-em)]PDI = 0.054, PBS[thin space (1/6-em)]:[thin space (1/6-em)]PDI = 0.102), indicating the homogeneous distribution of the liposomes in the medium.

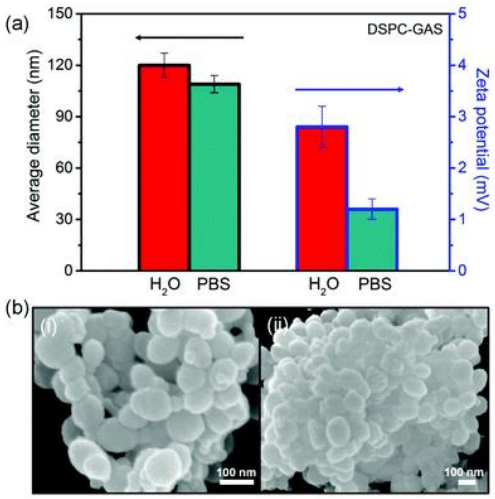

Fig. 1 Characterization of DSPC–GAS liposomes prepared with the molar ratio of 2 : 8 at the DSPC concentration of 5.0 mM. (a) The average diameters and zeta potentials at 37 °C. (b) SEM images in different media: (i) H_2O, (ii) PBS.

Fig. 1b shows the SEM images of DSPC–GAS liposomes in H2O and PBS after adsorption onto silicon wafers. It can be observed that DSPC–GAS liposomes prepared in H2O and PBS both exhibited as self-closed liposomes on silicon wafers which demonstrated the robust stability of DSPC–GAS liposomes on the surface. Moreover, in terms of packing density, DSPC–GAS liposomes in H2O and PBS exhibited as clustered spherical liposomes on the silicon wafers. In general, the adsorption of the liposomes on the silicon wafers was due to the dipole–charge attraction between the zwitterionic headgroups exposed by the phosphocholine liposomes and the negatively charged silica surface. This statement was confirmed by the results from the SEM images of the DSPC–GAS liposomes in H2O and PBS. Additionally, in both media, the mean diameters of the DSPC–GAS liposomes on the surface appeared to be slightly smaller than those obtained by the DLS measurements of the liposomes in aqueous solution. This was due to the fact that the hydrodynamic diameter of DSPC–GAS liposomes measured by DLS included the hydration layer surrounding them, leading to increased size compared to that obtained using SEM.

3.3. GAS encapsulation efficiency in different media

On the basis of the selection for the optimized formulation for GAS loading, the loading capacity and encapsulation efficiency of DSPC–GAS liposomes in PBS prepared at the optimum molar ratio

in the DSPC concentration of 5.0 mM were obtained. It was found that both the loading capacity (36.0 ± 1.4%) and the encapsulation efficiency (61.6 ± 0.9%) of the DSPC–GAS liposomes in PBS were higher than those in H2O (LC% = 29.3 ± 1.2%, EE% = 50.1 ± 1.2%). This was likely due to the presence of the salts in PBS which enhanced the compactness of DSPC–GAS bilayers. When the DSPC–GAS liposomes were prepared in H2O, charge separation in DSPC headgroups led to repulsion between molecules, causing a decrease in packing of the bilayers. While in PBS, charge repulsion in DSPC headgroups was screened by salt ions, causing more compact bilayers and thus decreasing the leakage of GAS from DSPC–GAS liposomes during the preparation process.

3.4. GAS release behaviors and lubrication properties of the DSPC–GAS liposomes in different media

The GAS release behaviors and lubrication properties of DSPC–GAS liposomes prepared with the optimum molar ratio at the DSPC concentration of 5.0 mM in H2O and PBS at 37 °C were studied as follows. The DSPC–GAS liposomes were first dialyzed in two different media for 1 day via a dialysis tube (molecular weight cutoff: 1000). This was done prior to the GAS release and lubrication tests (please see results in Fig. 2).

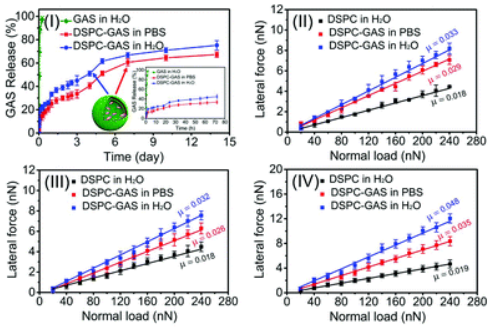

Fig. 2 GAS release and lubrication properties of the DSPC liposomes and the DSPC–GAS liposomes prepared with a 2 : 8 molar ratio at 5.0 mM DSPC concentration in H_2O and PBS at 37 °C. GAS release profiles (inset shows detailed GAS release profiles by 72 h.) (I); Lateral force as a function of normal load of the DSPC liposomes and the DSPC–GAS liposomes prepared after dialyzing for 1 (II), 3 (III) and 7 days (IV) at the scanning speed of 2.00 Hz.

3.4.1. GAS release from DSPC–GAS liposomes in different media. As shown in Fig. 2I, the release amount of 5.0 mM free GAS increased with time and a 97.2 ± 2.5% of GAS was observed in the solution within the first 2 h. In contrast, the GAS release curves of the DSPC–GAS liposomes in two media (H2O and PBS) both exhibited a sustained release profile characterized by a short initial burst release followed by a relatively stable release. The release amounts of GAS from the DSPC–GAS liposome in H2O and PBS within 2 h were 19.1 ± 2.2% and 12.6 ± 3.2%, respectively. Compared to the free GAS control group, the release of GAS from DSPC–GAS liposomes in H2O and PBS was both prolonged to 14 days. Moreover, it was found that the GAS release rate in PBS was lower than that in H2O during the measuring period. Specifically, 33.5 ± 3.5% and 44.9 ± 4.2% GAS were released from the DSPC liposomes in PBS and H2O after 72 h, respectively (inset in Fig. 2I). This result was attributed to the fact that the electrostatic binding between the salt ions in PBS and the oppositely charged headgroups of the lipid molecules resulted in a tighter packing of the DSPC–GAS liposomes, and therefore a decrease in permeability to inhibit GAS release. The same argument also applied to the salt-modified compactness for the loading capacity and encapsulation efficiency of the DSPC–GAS liposomes in PBS. The combined results of GAS loading and release indicated that enhanced compactness of the DSPC–GAS liposomes in PBS contributed to a greater

encapsulation efficiency and lower GAS release.

3.4.2. Lubrication properties of the DSPC–GAS liposomes in different media. With regard to GAS released from the DSPC–GAS liposomes in H2O and PBS, the salt effects on the compactness of these samples were discussed. The DSPC–GAS liposomes prepared with the two media were selected to further investigate the effects of salts on their lubrication properties. The two solutions were studied by an Asylum Research MFP-3D AFM in contact mode. Fig. 2II, III and IV show the lateral force (FL) against the normal force (FN) between the silica surface and polystyrene surface bearing an adsorbed layer formed by 30 min of adsorption from the DSPC–GAS liposomes in both media. The DSPC–GAS liposomes used were separately prepared after dialyzing for 1, 3 and 7 days via a dialysis tube (molecular weight cut-off: 1000) at 5.0 mM and 37 °C. The lubrication properties of the DSPC liposomes prepared in H2O and PBS were also investigated as a control and similar friction behavior was observed (Fig. S3a†). Hence, the results for the DSPC liposomes prepared in H2O under the same conditions were used for further comparison. The corresponding friction results for the samples dialyzed for 14 days are given in Fig. S3b.† As shown in Fig. 2II, the friction measurements were performed over a normal force range of 20–240 nN, while the scanning speed was set as 2.00 Hz. When examining the DSPC–GAS liposomes prepared after dialyzing for 1 day, the lateral force between the silica surface and the polystyrene surface increased linearly upon increasing the normal load. Through linear fitting to FL–FN points, the corresponding friction coefficients were obtained. The friction coefficients of the DSPC–GAS liposomes in H2O and PBS were $\mu = 0.033$ and 0.029 by fitting the experimental points, which were significantly lower than the friction coefficients of water and HA (5.0 mg mL−1) ($\mu = 0.350$ and 0.168, Fig. S5†). Such linear relationship between the lateral force and the normal force was also observed in the case of DSPC liposomes in H2O and PBS. However, the friction coefficients ($\mu = 0.018$ and 0.017) obtained from the DSPC liposomes in H2O and PBS were smaller than those obtained from DSPC–GAS liposomes in H2O and PBS. This was likely due to the fact that SO_4^{2-} from the released GAS from the DSPC–GAS liposomes created a bridging effect among the adjacent liposomes, leading to the formation of nonuniform adsorbed layers and thus a higher friction coefficient.45 In addition, comparison between the friction coefficients obtained with the DSPC–GAS liposomes in H2O and PBS demonstrated that they were both quite similar, however, the friction coefficient in H2O was slightly larger than that in PBS. This was attributed to the electrostatic screening paired with the hydration lubrication of the hydrated salt ions in PBS, which had the opposite effects.46–48 The electrostatic screening induced a more compact and robust packing of the phospholipids in the DSPC liposomes, and thus an increased mechanical stability which contributed to the efficient boundary lubrication and a lower GAS release rate. The effect of the salt ions on the packing of the liposomes was previously reported by Sanz et al.49 to elucidate the friction properties of 1,2-dimyristoyl-sn-glycero-3-phosphocholine (DMPC) in a liquid environment. Therefore, this study further supports the importance of mechanical stability as a contributor to the effective lubrication of liposomes. Meanwhile, the salt-induced lower GAS release in PBS decreased the release amount of SO_4^{2-} from the DSPC–GAS liposomes, leading to a weaker bridging effect on the DSPC liposomes and thus a lower friction coefficient. In contrast, the hydration lubrication of the salt ions reduced the hydration extent of the DSPC liposomes and increased the friction coefficient by competing with the phospholipid headgroups for water of hydration. Either interaction played a dominant role in determining the lubrication behaviors of the DSPC–GAS liposomes in PBS. Upon further analysis of the DSPC–GAS liposomes prepared after dialyzing for 3 and 7 days, it was found

that there were similar friction results except for the higher friction coefficients (Fig. 2III and IV). The friction coefficient increased with the increase of dialysis time of the DSPC–GAS liposomes. Regardless, the friction coefficients of the DSPC–GAS liposomes dialyzed for 14 days in H2O and PBS (μ = 0.165 and 0.123) were still lower than those of water and HA (5.0 mg mL−1) under the same conditions. This information indicates that the DSPC–GAS liposomes prepared by dialyzing over a 14 day period at 37 °C still had a lubrication effect between the silica surface and polystyrene surface upon load application. The results also suggest the potential of the DSPC–GAS liposomes as efficient boundary lubricants for reducing the frequency of administration when being intra-articularly injected into the joint capsules.

As noted in Fig. S3b,† the DSPC–GAS liposomes prepared under two different media after dialyzing for 14 days at 37 °C still had a lubrication effect upon application of the load. Moreover, the different media used in the study played an important role in the stability of the DSPC–GAS liposomes, and in the lubrication properties. To provide insight into the stability and durability of the liposome layer, the lateral forces of the DSPC–GAS liposomes (molar ratio of 2[thin space (1/6-em)]:[thin space (1/6-em)]8, 5.0 mM) prepared in H2O and PBS against different normal loads under four different scanning speeds (1.00, 2.00, 3.91 and 7.81 Hz) and against cycles in the same scanning area were measured. The representative results for the DSPC–GAS liposomes prepared after dialyzing for 1 day are shown in Fig. 3.

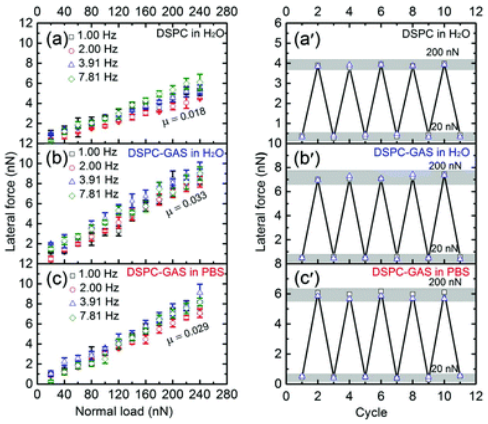

Fig. 3 Lateral force as a function of normal load of the DSPC liposomes and the DSPC–GAS liposomes prepared after dialyzing for 1 day under four different scanning speeds (1.00, 2.00, 3.91 and 7.81 Hz) (a–c) and of cycle under a high load (F_N = 200 nN) and a low load (F_N = 20 nN) at the scanning speed of 2.00 Hz (a′–c′). Data from runs at two different positions with five steps (from increasing load to reducing load as one step) were shown.

Firstly, when looking at the situation for the lubrication properties of the DSPC–GAS liposomes under different scanning speeds which can be seen in Fig. 3b and c, both H2O and PBS had almost the same lubrication behaviors of the DSPC–GAS liposomes under the four different scanning speeds. Moreover, the lateral force slightly fluctuated with variations in scanning speed from 1.00 to 7.81 Hz. The friction coefficients of the DSPC–GAS liposomes in each medium were almost unchanged under these four different speeds. This indicated that the friction coefficient in the range of the normal load studied was independent of the scanning speed. These results demonstrated that the lubrication of the DSPC–GAS liposomes in H2O and PBS acted as boundary lubrication. Similar friction results were also observed in the case of the DSPC liposomes in H2O (Fig. 3a), demonstrating the little effect of the released GAS from the DSPC–GAS liposomes on the

lubrication mechanism. This argument was further supported by the lubrication results obtained with the DSPC–GAS liposomes prepared after dialyzing for 3, 7 and 14 days (Fig. S4†).

Another aspect to be addressed is the mechanical stability of the DSPC–GAS liposomes in different media. As shown in Fig. 3a′–c′, when the steps of the friction measurements (from increasing load to reducing load) were repeated five times in the same scanning area, the lateral force of the DSPC and the DSPC–GAS liposomes in each medium had constant values when under both high loads (FN = 200 nN) and low loads (FN = 20 nN). This indicated that either the DSPC liposomes or the DSPC–GAS liposomes had very good stability and reversibility with friction.

Taken together, the above results indicated that the DSPC–GAS liposomes in both media demonstrated sustained GAS release behaviors, and displayed good lubrication properties with regard to reversibility and durability under the applied load. This can be attributed to the stability of the compact liposomes. In brief, the higher the mechanical stability, the lower the release rate and better the lubrication capability.

3.4.3. Effect of different media on the intermolecular interactions. As mentioned above, GAS release from the DSPC–GAS liposomes demonstrated a sustained release with a lower release rate observed in PBS when compared to H2O. Meanwhile, the lubrication ability of the DSPC–GAS liposomes in PBS was superior to that of H2O. In general, it is important to note that the drug release from liposomes was related to the stability of liposomes,50 which was related to the intermolecular interactions, such as electrostatic interaction and hydrophobic interaction. In the case of PBS, salts affected the stability of the DSPC–GAS liposomes by tuning the electrostatic interaction between the salt ions in PBS and the oppositely charged headgroups of the lipid molecules in liposomes.51 The addition of salt ions decreased the repulsion effect between the lipid molecules caused by the charge separation in DSPC polar heads, and thus increased the packing of the DSPC–GAS bilayers. Consequently, the DSPC liposomes became more stable which in turn caused a decrease in GAS release. The argument in terms of salt effect on the stability of the DSPC–GAS liposomes also applied to the lubrication properties, as the salt-enhanced stability contributed to not only an efficient boundary lubrication but also a lower SO_4^{2-} release amount, which weakened the bridging effect of SO_4^{2-}, and thus decreased the formation and breakage of charge–dipole bonds between SO_4^{2-} and DSPC headgroups, resulting in a lower friction coefficient. Additionally, the hydration lubrication of hydrated salt ions also played a role in the lubrication properties, due to the fact that the competition of hydrated salt ions for the water of hydration reduced the efficiency of the hydration lubrication mechanism for DSPC liposomes.

In summary, the GAS release behaviors and lubrication properties of the DSPC–GAS liposomes indicated that the salts mainly affected the release properties and the lubrication capability through tuning the electrostatic interaction, and the enhanced electrostatic interaction helped to stabilize the DSPC–GAS liposomes. On the basis of the aforementioned results and mechanism, the salt effects on the GAS release behaviors and the lubrication properties of the DSPC–GAS liposomes are summarized in a schematic illustration (Fig. 4).

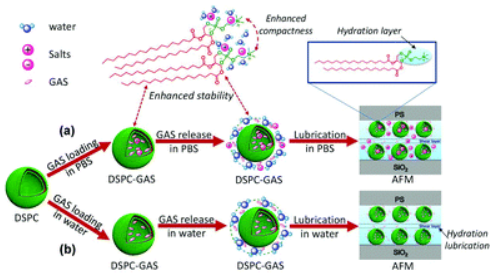

Fig. 4 Mechanism of the sustained drug release and the improved lubrication of the DSPC–GAS liposomes in different media (H_2O and PBS): (a) In the presence of salts, the salt ions in PBS and the oppositely charged headgroups of the lipid molecules interacted electrostatically, leading to a more compact packing of the DSPC liposomes; (b) DSPC–GAS liposomes were prepared in H_2O.

3.5. Cytotoxicity and protective effect for inflammation induced degeneration of chondrocytes

As mentioned above, the DSPC–GAS liposomes as drug nanocarriers provided a combination of sustained drug release and lubrication improvement. Next, we discussed whether the GAS release could suffice for the therapeutic efficacy of OA. In view of the total GAS release amount (10.0 mM) in the DSPC–GAS liposomes, which is much higher than the amount used to increase the protein synthesis (50 μM or higher) and Agg mRNA level (50–200 μM), together to inhibit the activity of MMPs, it is therefore useful to investigate the cytotoxicity and protective effect for inflammation-induced degeneration of chondrocytes to examine the feasibility of applying DSPC–GAS liposomes for the treatment of OA.52,53

3.5.1. Effect of the DSPC–GAS liposomes on the chondrocyte viability and proliferation. The Live/Dead assay in addition to the CCK-8 test was performed to investigate the cytotoxicity effect of the DSPC–GAS liposomes on the viability and proliferation of primary mouse chondrocytes. Meanwhile, the cytotoxicity effect of both DSPC liposomes and free GAS solution at 5.0 mM was investigated as the control groups. As can be seen in Fig. 5, after incubation for 1, 3 and 5 days, the Live/Dead assay displayed the morphologies of viable and dead cells after staining with the Live/Dead cell dye. The intuitive results demonstrated that most of the seeded mouse chondrocytes in the DSPC–GAS group stayed alive over the course of 5-day culture and the cell density increased gradually with time from day 1 to day 5 (Fig. 5a). We found that the viability of chondrocytes in the DSPC–GAS group was almost the same as the control (PBS) group for all incubation times, indicating that the DSPC–GAS liposomes had no detrimental effect on the chondrocytes. In addition, the CCK-8 assay displayed that both the DSPC group and the GAS group had no cytotoxicity compared to the control (PBS) group. Moreover, the DSPC–GAS group slightly enhanced the proliferation of the chondrocytes compared to that of the control (PBS) group, DSPC group and free GAS group on the third day (Fig. 5c). To briefly summarize the findings listed above, both Live/Dead and CCK-8 assay suggested that the DSPC–GAS liposomes exhibited no cytotoxicity and excellent biocompatibility to the viability and proliferation of chondrocytes.

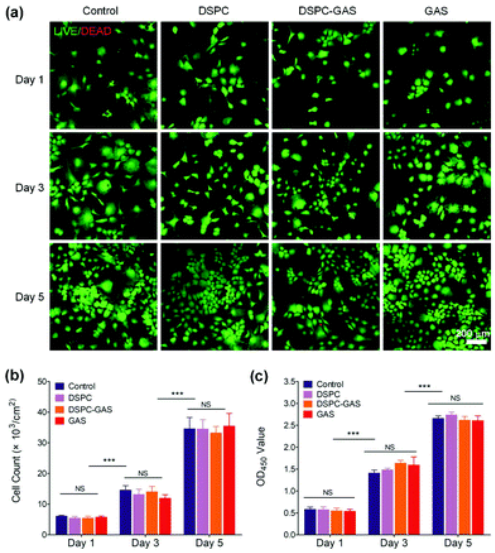

Fig. 5 (a) Viability of chondrocytes cultured with the control (PBS), DSPC, DSPC–GAS liposomes or 5.0 mM GAS at different time points, detected using fluorescence microscopy. Live cells were stained green and dead cells stained red; (b) Cell count of chondrocytes which were viable when incubated with the control (PBS), DSPC, DSPC–GAS liposomes or 5.0 mM GAS for 1, 3 and 5 days. (c) Proliferation of control (PBS), DSPC, DSPC–GAS liposomes or 5.0 mM GAS on primary mouse chondrocytes examined with CCK-8. $n = 3$; NS = no significance; $^{***}P < 0.001$.

3.5.2. Effect of the DSPC–GAS liposomes on the mRNA expression in mouse chondrocytes treated with TNF-α. The pathogenesis of OA was taken into consideration and integrated in multiple factors, such as mechanical loading stress, inflammatory factors and MMPs, which can lead to chondrocyte degeneration as well as OA. TNF-α, a pro-inflammatory cytokine, plays an important role in OA as it is a principle inflammatory component as well as a destructive component. In this study, we introduced TNF-α to investigate the anti-inflammatory and chondroprotective potential of the DSPC–GAS liposomes via the production variations of six molecules related to the course of OA development such as IL-1β, IL-6, TAC1, MMP1, Agg and Col2α by the primary mouse chondrocytes. A compilation of the results about the inflammation-induced degeneration of chondrocytes obtained by QRT-PCR analyses are collected in Fig. 6. The primary mouse chondrocytes were either treated or not treated with TNF-α (5 nM) and then cultured with the DSPC or DSPC–GAS liposomes (1.0 and 5.0 mM), or free GAS solution (5.0 mM) for 24 h. Fig. 6a and b show the effect of the DSPC–GAS liposomes on the TNF-α-induced mRNA expression of IL-1β and IL-6. Elevated levels of IL-1β and IL-6, which contributed to the cartilage degeneration by its induction of proteoglycan loss and matrix degradation, occurred in the synovial fluid and cartilage tissue of patients with OA. Upon further analysis, treatment with TNF-α significantly increased the mRNA expression of IL-1β (4.7-fold; $p < 0.001$) and IL-6 (4.4-fold; $p < 0.001$) compared to the untreated control group. Particularly, TNF-α-induced mRNA expression of IL-1β (33.8%; $p < 0.05$) and IL-6 (25.3%; $p < 0.01$) was separately inhibited by the culture with 5.0 mM DSPC–GAS liposomes compared to the TNF-α-treated blank group. Between the DSPC–GAS groups, the inhibition effect of DSPC–GAS at 5.0 mM was greater than that of 1.0 mM, however, smaller than that of 5.0 mM free GAS. The discrepancies in the TNF-α-induced mRNA expression of IL-1β and IL-6 were attributed to the dose-dependent therapeutic efficacy of GAS. Due to the slow release rate of GAS from the DSPC–GAS liposomes, the concentrations of GAS in both DSPC–GAS groups (1.0 and 5.0 mM) during chondrocyte culture were lower than that in the free GAS group. Therefore,

the inhibition effect of DSPC–GAS at 5.0 mM on IL-1β and IL-6 expression was higher compared to that of 1.0 mM, but lower compared to that of 5.0 mM free GAS. In contrast, there was no significant difference in the mRNA expression of IL-1β and IL-6 for the chondrocytes cultured with the DSPC liposomes at 1.0 and 5.0 mM respectively. These results indicated that DSPC–GAS liposomes reduced the production of IL-1β and IL-6 for TNF-α treated chondrocytes and the anti-inflammatory effect of the DSPC–GAS liposomes was enhanced at higher concentrations.

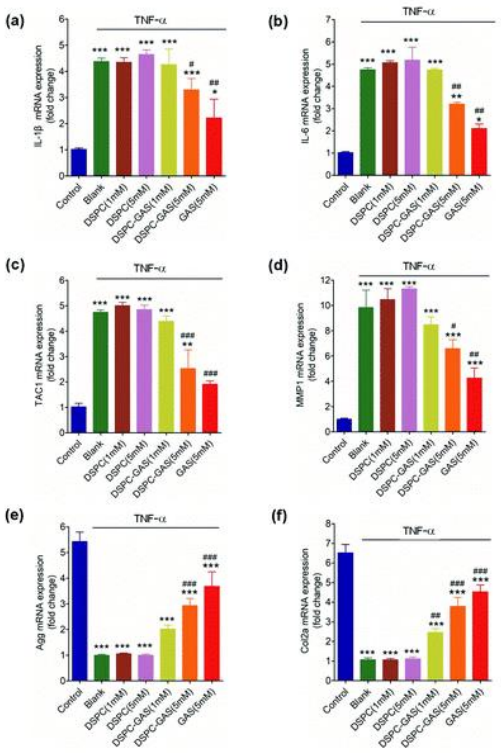

Fig. 6 QRT-PCR analysis for the mRNA expression of IL-1β (a), IL-6 (b), TAC1 (c), MMP1 (d), Agg (e) and Col2α (f) in chondrocytes treated with 5 nM TNF-α and cultured with the DSPC, DSPC–GAS liposomes or free GAS for 24 h. $n = 3$, $^{*}P < 0.05$, $^{**}P < 0.01$, $^{***}P < 0.001$, compared with control groups; $^{\#}P < 0.05$, $^{\#\#}P < 0.01$, $^{\#\#\#}P < 0.001$, compared with the blank groups.

We then investigated the impact of the treatment with the DSPC–GAS liposomes on the mRNA expression of TAC1 and MMP1 of TNF-α treated chondrocytes. On a side note, it is important to note that TAC1, a pain related gene, involves in the regulation of pathological processes of OA while MMP1 contributes to the cartilage degeneration and metastasis. As shown in Fig. 6c and d, TNF-α-treated chondrocytes resulted in a significant up-regulation of TAC1 (4.9-fold; $p < 0.001$) and MMP1 (9.5-fold; $p < 0.001$) mRNA expression. The culture of TNF-α-treated chondrocytes with the DSPC–GAS liposomes (5.0 mM) showed a noticeable decrease in the mRNA expression level of TAC1 (46.2%; $p < 0.001$) and MMP1 (30.7%; $p < 0.05$), whereas the culture of TNF-α-treated chondrocytes with the DSPC liposomes (1.0 and 5.0 mM) showed a slight increase in the mRNA expression level for both TAC1 and MMP1, compared to the TNF-α-treated blank group. As to the free GAS group, the down-regulation of TAC1 and MMP1 was still greater than that of the DSPC–GAS groups. When all the above results were taken into consideration, it was clear to conclude that the addition of DSPC–GAS liposomes reduced the production of pain related gene expression (TAC1) and catabolism proteases (MMP1) of the TNF-α treated chondrocytes.

To demonstrate the cartilage protective ability of the DSPC–GAS liposomes, we further explored their effect on the mRNA expression of Agg and Col2α in chondrocytes treated with TNF-α. Agg and Col2α are important components of ECM, as they are required for the cartilage regeneration and repair. In addition, down-regulation of Agg and Col2α will lead to progressive cartilage degeneration. As shown in Fig. 6e and f, TNF-α induction resulted in a significant down regulation of Agg (79.3%; $p < 0.001$) and Col2α (83.7%; $p < 0.001$) mRNA expression when compared to the untreated control group. The culture of TNF-α-treated chondrocytes with the DSPC–GAS liposomes (5.0 mM) produced a significant increase in the mRNA expression level of Agg (64.9%; $p < 0.001$) and Col2α (75.0%; $p < 0.001$), though the increase in the trend was less than that of the free GAS groups. On the other hand, the culture of TNF-α-treated chondrocytes with the DSPC liposomes (1.0 and 5.0 mM) exerted no obvious influence on the mRNA expression level of both Agg and Col2α, compared to the TNF-α-treated blank group. The elevated levels of both Agg and Col2α are manifestations of healthy chondrocytes, therefore, the results indicated that the DSPC–GAS liposomes displayed the chondroprotective potential in inflammation-induced chondrocytes.

3.5.3. Effect of the DSPC–GAS liposomes on the protein expression in mouse chondrocytes treated with TNF-α. An immunofluorescence staining analysis was performed to study the effects of the DSPC–GAS liposomes on the protein expression of Col2α and MMP1 in mouse chondrocytes treated with TNF-α. The chondrocytes were treated with 5 nM TNF-α and 5.0 mM of DSPC, DSPC–GAS liposomes or free GAS solution for 12 h. As shown in Fig. 7a and Fig. S6a,† TNF-α-treated chondrocytes in the blank group displayed weak Col2α staining intensity, while the culture of TNF-α-treated chondrocytes with the DSPC–GAS liposomes demonstrated a strong Col2α staining intensity. The results supported the conclusion that the addition of the DSPC–GAS liposomes reversed TNF-α-treated reduction of Col2α protein expression. Fig. 7a and Fig. S6b† also showed that TNF-α significantly increased MMP1 expression at the protein level, whereas the culture with the DSPC–GAS liposomes reversed the effect of TNF-α on MMP1 protein expression. Collectively, the results demonstrated that the DSPC–GAS liposomes increased the production of anabolic protein expression (Col2α) and decreased the production of catabolic protein expression (MMP1) of TNF-α treated chondrocytes, which were further quantitatively confirmed by their corresponding statistical analysis (Fig. 7b).

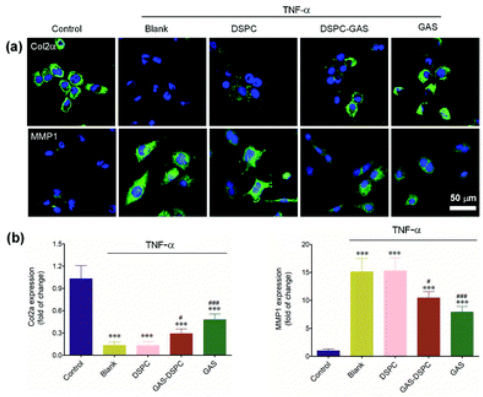

Fig. 7 (a) Representative photomicrographs of chondrocytes treated with 5 nM of TNF-α, and cultured with DSPC, DSPC–GAS liposomes or free GAS for 12 h, acquired using laser scanning confocal microscopy. Green: Alexa Fluor (488) labelling Col2α or MMP1; blue: DAPI labeling cell nuclei. (b) The quantitative data showing comparison of Col2α or MMP1 protein expression of chondrocytes treated with 5 nM of TNF-α, and co-cultured with DSPC, DSPC–GAS liposomes or free GAS for 12 h. $n = 3$, $^{***}P < 0.001$, compared with control groups; $^{\#}P < 0.05$, $^{\#\#\#}P < 0.001$, compared with the blank groups.

As discussed previously, we demonstrated that the anti-inflammatory effect of the DSPC–GAS liposomes through inhibition of the pro-inflammatory cytokine TNF-α, which caused the increase of the mRNA expression of two other pro-inflammatory cytokines (IL-1β and IL-6) as well as the expression of pain related gene and catabolism protease (TAC1 and MMP1) associated with cartilage degradation. We also outlined the chondroprotective ability of the DSPC–GAS liposomes through upregulating cartilage anabolic factors (Agg and Col2α) in the TNF-α-treated chondrocytes. Moreover, the chondroprotective ability of the DSPC–GAS liposomes was confirmed by the fact that the DSPC–GAS liposomes contributed to the increase of anabolic protein expression in TNF-α-treated chondrocytes. The combined results suggest that there is a protective effect of the DSPC–GAS liposomes for inflammation-induced degeneration of chondrocytes, as well as outline the potential clinical application for OA treatment.

4. Conclusions

The present work systematically examines the drug release behaviors and lubrication properties of the GAS-loaded DSPC liposomes in two different media which include H2O and PBS, and their anti-inflammatory and chondroprotective potential in inflammation-induced chondrocytes. Firstly, GAS released from the DSPC–GAS liposomes in H2O and PBS at 37 °C was studied in detail, and the sustained release of the GAS was observed under both conditions. Moreover, a lower release of GAS was observed in PBS when compared to that in H2O. This result occurred because of the electrostatic binding between the salt ions in PBS and the oppositely charged headgroups of the lipid molecules, which led to a denser packing of the DSPC liposomes and thus decreased their permeability. Next, the lubrication properties of the GAS-loaded DSPC liposomes prepared in the two media at 37 °C were studied. These DSPC–GAS liposomes were highly stable under H2O and PBS with the applied load and provided good lubrication. Moreover, the DSPC–GAS liposomes prepared in PBS achieved a lower friction coefficient when compared to the other groups. The lubrication results obtained by using different media can be elucidated by the salt-induced variations in the electrostatic interaction of the headgroup area based on the hydration lubrication mechanism. Lastly, the DSPC–GAS liposomes were biocompatible and provided a protective effect for

inflammation-induced degeneration of chondrocytes. This investigation provides an effective strategy to treat OA using a combination of sustained drug release and lubrication improvement.

Conflicts of interest

The authors declare no competing financial interest.

Acknowledgements

This work was financially supported by the National Natural Science Foundation of China (grant no. 51675296 and 11732015), the Ng Teng Fong Charitable Foundation (grant no. 202-276-132-13), the Tsinghua University Initiative Scientific Research Program (grant no. 20151080366), and the Research Fund of State Key Laboratory of Tribology, Tsinghua University, China (grant no. SKLT2018B08) and the start-up fund (1-ZE7S) and central research fund (G-YBWS) from the Hong Kong Polytechnic University.

References

1 J. Knoop, J. Dekker, J. P. Klein, M. Leeden, M. Esch, D. Reiding, R. E. Voorneman, M. Gerritsen, L. D. Roorda, M. P. M. Steultjens and W. F. Lems, Arthrit. Res. Ther., 2012, 14, R212

2 N. Gerwin, C. Hops and A. Lucke, Adv. Drug Deliv. Rev., 2006, 58, 226-242.

3 Q. Wang and X. Sun, Biomater. Sci., 2017, 5, 1407-1420.

4 L. E. Tellier, E. A. Trevino, A. L. Brimeyer, D. S. Reece, N. J. Willett, R. E. Guldberg and J. S. Temenoff, Biomater. Sci., 2018, 6, 1159-1167.

5 S. Ghanbarzadeh and S. Arami, Biomed. Res. Int., 2013, 2013, 616810.

6 V. P. Torchilin, Nat. Rev. Drug Discov., 2005, 4, 145-160.

7 D. Dyondi, A. Sarkar and R. Banerjee, J. Biomed. Nanotechnol., 2015, 11, 1225-1235.

8 A. Sharma and S. Arora, World J. Pharm. Pharm. Sci., 2013, 2, 6448-6462.

9 G. M. Ngandeu Neubi, Y. Opoku-Damoah, X. Gu, Y. Han, J. Zhou and Y. Ding, Biomater. Sci., 2018, 6, 958-973.

10 Z. Fan, J. Li, J. Liu, H. Jiao and B. Liu, ACS Appl. Mater. Interfaces, 2018, 10, 23595-23604.

11 T. A. Holland and A. G. Mikos, J. Control. Release, 2003, 86, 1- 14.

12 E. Horisawa, T. Hirota, S. Kawazoe, J. Yamada, H. Yamamoto, H. Takeuchi and Y. Kawashima, Pharm. Res., 2002, 19, 403- 410.

13 Q. Zhang, D. Dehaini, Y. Zhang, J. Zhou, X. Chen, L. Zhang, R. H. Fang, W. Gao and L. Zhang, Nat. Nanotechnol., 2018, DOI: 10.1038/s41565-018-0254-4.

14 W. Scarano, P. de Souza and M. H. Stenzel, Biomater. Sci., 2015, 3, 163-174.

15 Q. L. Li, Y. Sun, Y. L. Sun, J. Wen, Y. Zhou, Q. M. Bing, L. D. Isaacs, Y. Jin, H. Gao and Y. W. Yang, Chem. Mater., 2014, 26, 6418-6431.

16 J. Zhang, Z. F. Yuan, Y. Wang, W. H. Chen, G. F. Luo, S. X. Cheng, R. X. Zhuo and X. Z. Zhang, J. Am. Chem. Soc., 2013, 135, 5068-5073.

17 A. Watermann and J. Brieger, Nanomaterials, 2017, 7, 189.

18 M. Tuncay, S. Calis, H. S. Kas, M. T. Ercan, I. Peksoy and A. A. Hincal, J. Microencapsul., 2000, 17, 145-155.

19 X. Zhao, C. Hu, G. Pan and W. Cui, Part. Part. Syst. Charact., 2015, 32, 529-535.

20 X. Zhao, J. Zhao, Z. Y. Lin, G. Pan, Y. Zhu, Y. Cheng and W. Cui, Colloids Surf. B. Biointerfaces, 2015, 130, 1-9.

21 X. Zhao, Z. Yuan, L. Yildirimer, J. Zhao, Z. Y. Lin, Z. Cao, G. Pan and W. Cui, Small, 2015, 11, 4284-4291.
22 J. H. Ratcliffe, I. M. Hunneyball, C. G. Wilson, A. Smith and S. S. Davis, J. Pharm. Pharmacol., 1987, 39, 290-295.
23 A. Duro-Castano, J. Movellan and M. J. Vicent, Biomater. Sci., 2015, 3, 1321-1334.
24 M. Wang and Z. Peng, Wear, 2015, 324-325, 74-79.
25 Y. Sun, H. Zhang, Y. Wang and Y. Wang, J. Controlled Release, 2017, 259, e45-e46.
26 T. Sun, Y. Sun and H. Zhang, Polymers, 2018, 10, 513.
27 R. Goldberg and J. Klein, Chem. Phys. Lipids, 2012, 165, 374- 381.
28 S. Sivan, A. Schroeder, G. Verberne, Y. Merkher, D. Diminsky, A. Priev, A. Maroudas, G. Halperin, D. Nitzan, I. Etsion and Y. Barenholz, Langmuir, 2010, 26, 1107-1116.
29 Y. Duan, Y. Liu, C. Zhang, Z. Chen and S. Wen, Langmuir, 2016, 10957-10966.
30 U. Raviv and J. Klein, Science, 2002, 297, 1540-1543.
31 T. Viitala, J. T. Hautala, J. Vuorinen and S. K. Wiedmer, Langmuir, 2007, 23, 609-618.
32 C. Rossi, E. Briand, P. Parot, M. Odorico and J. Chopineau, J. Phys. Chem. B, 2007, 111, 7567-7576.
33 H. S. Vasiliadis and K. Tsikopoulos, World J. Orthop., 2017, 8, 1-11. 34 M. E. Adams, Lancet, 1999, 354, 353-354. 35 J. W. Anderson, R. J. Nicolosi and J. F. Borzelleca, Food Chem. Toxicol., 2005, 43, 187-201.
36 J. Y. Reginster, R. Deroisy, L. C. Rovati, R. L. Lee, E. Lejeune, O. Bruyere, G. Giacovelli, Y. Henrotin, J. E. Dacre and C. Gossett, Lancet, 2001, 357, 251-256.
37 L. Zhu, J. Seror, A. J. Day, N. Kampf and J. Klein, Acta Biomater., 2017, 59, 283-292.
38 R. Sorkin, N. Kampf, Y. Dror, E. Shimoni and J. Klein, Biomaterials, 2013, 34, 5465-5475.
39 D. Lichtenberg and Y. Barenholz, Methods Biochem. Anal., 1988, 33, 337-462.
40 Y. Ni, C. Huang and S. Kokot, Anal. Chim. Acta, 2003, 480, 53- 65.
41 C. P. Green, H. Lioe, J. P. Cleveland, R. Proksch, P. Mulvaney and J. E. Sader, Rev. Sci. Instrum., 2004, 75, 1988-1996.
42 A. J. Mirando, R. Dong and J. Kim, Methods Mol. Biol., 2014, 267-277.
43 C. Li, K. Chen, H. Kang, Y. Yan, K. Liu, C. Guo, J. Qi, K. Yang, F. Wang, L. Guo, C. He and L. Deng, Cell Death Dis., 2017, 8, e3165.
44 K. J. Livak and T. D. Schmittgen, Methods, 2001, 25, 402-408.
45 A. Gaisinskaya-Kipnis, S. Jahn, R. Goldberg and J. Klein, Biomacromolecules, 2014, 15, 4178-4186.
46 J. Klein, Friction, 2013, 1, 1-23.
47 J. Seror, L. Zhu, R. Goldberg, A. J. Day and J. Klein, Nat. Commun., 2015, 6, 6497.
48 S. Jahn, J. Seror and J. Klein, Annu. Rev. Biomed. Eng., 2016, 18, 235-258.
49 G. Oncins, G. Garcia-Manyes and F. Sanz, Langmuir, 2005, 21, 7373-7379.
50 A. Tarasova, H. J. Griesser and L. Meagher, Langmuir, 2008, 24, 7371-7377.
51 E. Drinkel, F. D. Souza, H. D. Fiedler and F. Nome, Curr. Opin. Colloid Interface Sci., 2013, 18, 26-34.
52 M. Piperno, P. Reboul, M. P. H. Le Graverand, M. J. Peschard, M. Annefeld, M. Richard and E. Vignon, Osteoarthr. Cartilage, 2000, 8, 207-212.
53 G. R. Dodge and S. A. Jimenez, Osteoarthr. Cartilage, 2003, 11, 424-432.